ELSEVIER

Thermochimica Acta 340–341 (1999) 89–103

thermochimica acta

www.elsevier.com/locate/tca

Solid–liquid diffusion controlled rate equations

C.F. Dickinson[a,*], G.R. Heal[b]

[a]*Melting Technology, Pilkington Technology Centre, Hall Lane, Ormskirk, Lancs L40 5UF, UK*
[b]*Department of Chemistry and Applied Chemistry, University of Salford, The Crescent, Salford M5 4WT, UK*

Accepted 6 August 1999

Abstract

The paper is concerned with diffusion controlled reaction mechanisms and the associated rate equations. A review of previously reported rate equations was carried out and reported with the proofs of the equations. Three new rate equations are proposed based on the reaction of a solid and a liquid phase. Isothermal and non-isothermal experimental data was obtained for the reaction of sodium carbonate and calcium silicate and the data analysed to find the rate equation that best fitted the data. Isothermal data was analysed by reduced time plots and non-isothermal data was analysed by Šesták's method. One of the proposed equations provided a more perfect fit to the experimental data than any of the previously known rate equations.

While the experimental temperature suggested a solid–solid reaction mechanism, the experimental data gave a best fit with one of the proposed solid–liquid equations. An experimental method was devised to obtain mass loss data by TG on a rising temperature scale for liquid–solid phases without prior interaction in the solid–solid phase. The experimental data from this experiment could only result from a solid–liquid interaction and was shown to fit the same proposed rate equation as was observed in the solid–solid experiments.

It was concluded that a liquid phase was produced during the reaction at temperatures lower than might otherwise be expected.

Keywords: Kinetics; Diffusion; Thermogravimetric; Solid–liquid; Glass

1. Introduction

The reaction between sodium carbonate and calcium silicate was studied for its interest as a glass making reaction and was reported in the M.Sc. Thesis [1] of one of the authors. The reaction occurred in three distinct steps. Initially, the reaction appeared to be a solid state diffusion controlled acceleratory reaction. This was followed by a deceleratory reaction and finally by an acceleratory reaction. At first inspection it appeared logical that the reaction changes could be explained by the presence of a liquid sodium carbonate phase. However, there were certain observations which did not fit precisely with this simple model. It was observed that, the temperature where the reaction changed mechanism was slightly different at each heating rate chosen for the experiments. In fact, this temperature was lower when the heating rate was faster. It was found, also, that the mass loss data obtained from thermogravimetric measurements did not fit any of the accepted rate equations precisely. It was tempting to explain the temperature variation as being due to a thermal lag of the measured temperature. However, the authors familiarity with the equip-

*Corresponding author. Tel.: +44-0-1695-54236; fax: +44-0-1695-54506.
E-mail address: dickinsonc@pilkington.ptc.co.uk (C.F. Dickinson)

0040-6031/99/$ – see front matter
PII: S0040-6031(99)00256-7

ment persuaded him that this might not be the case and a more detailed investigation ensued.

2. Diffusion controlled reactions

A literature search for all kinetic equations has identified 25 equations in total and 9 of these are based on diffusion controlled mechanisms. Table 1 shows the diffusion controlled equations and Table 2 shows the other 16 equations. The notation used in the tables is that first suggested by Sharp et al. [2]. In addition to the equations cited in Sharp's paper, other equations have been suggested in the literature [3,4] and the authors have added these sequentially as they appeared. The literature revealed, also, that there were a number of discrepancies, equations were quoted which could not be identified nor could any proofs be found. The authors have assumed these to be typographical errors and have not included them. To the best of the authors beliefs, Tables 1 and 2 are an accurate, up to date collection of the known rate equations. The total number of equations that could be identified with certainty is 26. However, the Prout–Tompkins equation i.e. $kt = \ln(\alpha/1-\alpha)$, was not included in the computer programs because this equation could not be made to work with Šesták's method of analysis.

Table 1

Equation	Type	Notation
$kt = \alpha_2$	One-dimensional	D1
$kt = (1-\alpha)\ln(1-\alpha) + \alpha$	Two-dimensional	D2
$kt = [1-(1-\alpha)^{1/3}]^2$	Jander (three-dimensional)	D3
$kt = [1-(2\alpha/3)] - (1-\alpha)^{2/3}$	Ginstling–Brounshtein	D4
$kt = [1/(1-\alpha)^{1/3} - 1]^2$	Zhuravlev, Lesokhin and Templeman	D5
$kt = [(1+\alpha)^{1/3} - 1]^2$	'Anti-Jander' (three-dimensional)	D6
$k \ln t = [1-(1-\alpha)^{1/3}]^2$	Kröger and Ziegler	D7
$kt = [1-(1-\alpha)^{1/2}]^2$	Jander (cylindrical diffusion)	D8
$kt = [1-(1+\alpha)^{1/2}]^2$	'Anti-Jander' (cylindrical diffusion)	D9
$kt = ((1/(1-\alpha)^{1/3}) - 1)$	New equation	D10
$kt = (1/(1-\alpha)^{1/3} - 1) + 1/3\ln(1-\alpha)$	New equation	D11
$kt = 1/5(1-\alpha)^{-5/3} - 1/4(1-\alpha)^{-4/3} + 1/20$	New equation	D12

Table 2

Equation	Type	Notation
$kt = [-\ln(1-\alpha)]^{1/4}$	Avrami–Erofeev	A1
$kt = [-\ln(1-\alpha)]^{1/2}$	Avrami–Erofeev	A2
$kt = [-\ln(1-\alpha)]^{1/3}$	Avrami–Erofeev	A3
$kt = [-\ln(1-\alpha)]^{3/4}$	Avrami–Erofeev	A4
$kt = [-\ln(1-\alpha)]^{2/3}$	Avrami–Erofeev	A5
$kt = \alpha$	Zero order	F0
$kt = -\ln(1-\alpha)$	First order	F1
$kt = (1-\alpha)^{-1}$	Second order	F2
$kt = 1-(1-\alpha)^{1/2}$	Interface (contracting area)	R2
$kt = 1-(1-\alpha)^{1/3}$	Interface (contracting volume)	R3
$kt = 1-(1-\alpha)^{2/3}$	Interface	R4
$kt = \alpha_{1/2}$	Power law (half)	P1($n=2$)
$kt = \alpha_{1/3}$	Power law (third)	P1($n=3$)
$kt = \alpha_{1/4}$	Power law (quarter)	P1($n=4$)
$kt = \ln\alpha$	Exponential	E1
$kt = \exp(-(1-\alpha)) - \exp(-1)$	Exponential	E2
$kt = \ln[\alpha/(1-\alpha)]$	Prout–Tompkins[a]	B1

[a]Not included in computer programs.

The authors original analysis of the thermogravimetric data [1] using the 25 equations, was questionable because, although the D5 equation was the closest fit, the fit was not a perfect one and prompted a search for a more suitable equation. The reduced time analysis of the isothermal data identified the D5 diffusion controlled reaction mechanism equation as the closest fit to the experimental data. This equation was suggested by Zhuravlev et al. [3].

$$\left[\frac{1}{(1-\alpha)^{1/3}-1}\right]^2 = kt. \tag{1}$$

The equation is also referred to by Šesták et al. [5] who describe the equation as a modification of the Jander relation by assuming that the activity of the reacting substance was proportional to the fraction of un-reacted material $(1-\alpha)$. The theory is based on a process proceeding by instantaneous surface nucleation and the process being diffusion controlled. The suggested model assumes one of the reactants being spherical, of uniform radii and is surrounded by the other reactant. This is illustrated schematically in Fig. 1. Such models apply to reactions between solids and gases, solids and liquid and in certain solid–solid reactions if one of the reactants is considered as a continuous medium. In the diffusion controlled process one of the reactants must penetrate through the layer dividing the two reactants A and B.

Only the isothermal experiments could be described as being true example of a solid state reaction because of the complications introduced at a temperature of about 850°C when melting of the sodium carbonate occurred. Therefore the isothermal experiments were expected to give the most reliable identification of the reaction mechanism over the initial stages when the temperature was below 850°C. The results of the experiments, using the reduced time plots, indicated a reasonable fit to the Zhuravlev D5 model. However, as has been stated, it was significant that the experimental curves all lay on the same side of the ideal D5 plot away from all the other theoretical curves. Using different assumptions for the reaction processes it was possible to derive three additional equations that could be tested against the experimental data for a better fit. The assumptions and the derivation for the equations are set out below, starting from first principles to illustrate also the Jander, Kröger and Zhuravlev equations.

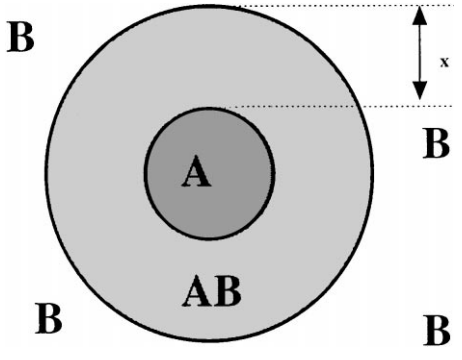

Fig. 1. Schematic representation of a solid in a sea of liquid (Solid A, Liquid B and Reaction layer AB).

Referring to Fig. 1, let the original radius be r_0. At time t the interface has spread inwards a distance x, leaving sphere of reactant A of radius r:

$$r = r_0 - x. \tag{2}$$

Volume of original sphere $= \frac{4}{3}\pi(r_0)^3$.

Volume of sphere at time t

$$= \tfrac{4}{3}\pi(r)^3 = \tfrac{4}{3}\pi(r_0-x)^3. \tag{3}$$

Value of fraction *un-reacted* on a *volume* basis is

$$(1-\alpha) = \frac{(4/3)\pi(r_0-x)^3}{(4/3)\pi(r_0)^3} = \frac{(r_0-x)^3}{(r_0)^3},$$

$$\therefore (1-\alpha)^{1/3} = \frac{r_0-x}{r_0} = 1-\frac{x}{r_0},$$

$$\therefore \frac{x}{r_0} = 1-(1-\alpha)^{1/3},$$

$$\therefore x = r_0\left(1-(1-\alpha)^{1/3}\right). \tag{4}$$

$$\frac{\mathrm{d}x}{\mathrm{d}\alpha} = \frac{1}{3}r_0(1-\alpha)^{-2/3}. \tag{5}$$

If the model is a diffusion controlled mechanism, a number of possible assumptions can be made to derive further rate equations.

Assuming the parabolic diffusion law, the following apply.

2.1. Diffusion equation D3

The time dependence of the gradual build up of the layer can be described by the parabolic law. Rate

varies inversely with x.

$$x^2 = 2DV_mC_0t = k_1t, \tag{6}$$

$$2\frac{x\mathrm{d}x}{\mathrm{d}t} = k_1 \quad \text{or} \quad \frac{\mathrm{d}x}{\mathrm{d}t} = \frac{k_1}{2x} = \frac{DV_mC_0}{x}, \tag{7}$$

where x is thickness of product layer, D the diffusion coefficient (slowest transport), V_m the volume of product AB formed from 1 mol of the slowest penetrating component, and C_0 the concentration of the penetrating species at the surface. From the above

$$x^2 = r_0^2\left(1-(1-\alpha)^{1/3}\right)^2 = k_1t,$$

$$\therefore \left(1-(1-\alpha)^{1/3}\right)^2 = \frac{k_1}{(r_0)^2}t = k't, \tag{8}$$

where $k' = (k_1/(r_0)^2)$.

Eq. (8) is the Jander equation for three dimensional diffusion type D3.

2.2. Diffusion equation D7

If the diffusion equation is

$$\frac{\mathrm{d}x}{\mathrm{d}t} = \frac{V_mC_0}{x}\frac{k_2}{t}. \tag{9}$$

(diffusion constant inversely proportional to t).

Integrate back again

$$\int 2x\mathrm{d}x = \int 2V_mC_0k_2\frac{\mathrm{d}t}{t},$$

$$x^2 = 2V_mC_0k_2\ln t.$$

$$\therefore r_0^2\left(1-(1-\alpha)^{1/3}\right)^2 = 2V_mC_0k_2\ln t$$

or

$$\left(1-(1-\alpha)^{1/3}\right)^2 = k_3\ln t, \tag{10}$$

which is the Kröger and Ziegler equation (D7) where

$$k_3 = \frac{2V_mC_0k_2}{r_0^2}.$$

2.3. Diffusion equation D8

Assume that the reacting species is cylindrical geometry and that the ends of the cylinder are inactive. Refer to Fig. 2.

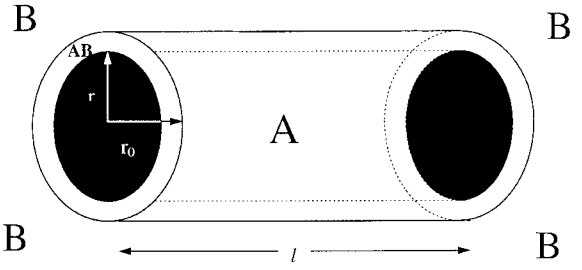

Fig. 2. Cylindrical reactant A surrounded by reactant B.

$$r = r_0-x.$$

Volume of original cylinder $= 2\pi r_0^2l$.

Volume of cylinder at time t

$$= 2\pi r^2l = 2\pi l(r_0-x)^2.$$

$$\text{The fraction un-reacted} = 1-\alpha = \frac{2\pi(r_0-x)^2}{2\pi r_0^2} = \frac{(r_0-x)^2}{r_0^2}.$$

$$(1-\alpha)^{1/2} = \frac{r_0-x}{r_0} = 1-\frac{x}{r_0},$$

$$\frac{x}{r_0} = 1-(1-\alpha)^{1/2},$$

$$x = r_0\left(1-(1-\alpha)^{1/2}\right),$$

$$\frac{\mathrm{d}x}{\mathrm{d}\alpha} = \frac{1}{2}r_0(1-\alpha)^{-1/2},$$

$$x^2 = r_0\left(1-(1-\alpha)^{1/2}\right)^2 \text{ from diffusion law} = kt,$$

$$\left(1-(1-\alpha)^{1/2}\right)^2 = \frac{k_1}{r_0^2} = k_1't. \tag{11}$$

This is the Jander equation for cylindrical diffusion D8.

2.4. Diffusion equation D9

Using the same geometric model as in Section 2.3, but assuming that the diffusion is outward from the cylinder A and that the product AB grows on the cylinder surface,

$$\alpha = \frac{(r_0+x)^2-r_0^2}{r_0^2} = \left(1+\frac{x}{r_0}\right)^2-1,$$

$$(1+\alpha) = \left(1+\frac{x}{r_0}\right)^2,$$

$$(1+\alpha)^{1/2} = 1 + \frac{x}{r_0},$$

$$(1+\alpha)^{1/2} - 1 = \frac{x}{r_0},$$

$$x^2 = r_0^2\left((1+\alpha)^{1/2} - 1\right)^2 = kt,$$

$$\left((1+\alpha)^{1/2} - 1\right)^2 = \frac{k_1}{r_0^2}t = k't. \tag{12}$$

This is the 'anti-Jander' equation for cylindrical diffusion D9.

2.5. Diffusion equation D5

Referring back to the spherical geometry in Fig. 1 and assume that the concentration C_0 is not a constant, but a factor of reactant activity varying with $(1-\alpha)$

$$\frac{\mathrm{d}x}{\mathrm{d}t} = \frac{DV_\mathrm{m}C_0(1-\alpha)}{x} = \frac{k_4(1-\alpha)}{x}, \tag{13}$$

where

$$k_4 = DV_\mathrm{m}C_0,$$

$$\therefore \frac{x\mathrm{d}x}{1-\alpha} = k_4\mathrm{d}t.$$

Substitute for x and $\mathrm{d}x$ from Eqs. (4) and (5) above,

$$\frac{r_0\left(1-(1-\alpha)^{1/3}\right)\times(1/3)r_0(1-\alpha)^{-2/3}}{1-\alpha}\mathrm{d}\alpha = k_4\mathrm{d}t,$$

$$\frac{(1/3)(r_0)^2\left((1-\alpha)^{-2/3} - (1-\alpha)^{-1/3}\right)\mathrm{d}\alpha}{1-\alpha} = k_4\mathrm{d}t,$$

$$\tfrac{1}{3}r_0^2\left((1-\alpha)^{-5/3} - (1-\alpha)^{-4/3}\right)\mathrm{d}\alpha = k_4\mathrm{d}t.$$

Integrate

$$\tfrac{1}{3}r_0^2\left(\tfrac{3}{2}(1-\alpha)^{-2/3} - 3(1-\alpha)^{-1/3} + c\right) = k_4 t,$$

at $t=0$, $\alpha=0$ then $c = 3/2$

$$r_0^2\left(\tfrac{1}{2}(1-\alpha)^{-2/3} - (1-\alpha)^{-1/3} + \tfrac{1}{2}\right) = k_4 t,$$

$$\tfrac{1}{2}r_0^2\left((1-\alpha)^{-2/3} - 2(1-\alpha)^{-1/3} + 1\right) = k_4 t,$$

$$\left((1-\alpha)^{-1/3} - 1\right)^2 = k_5 t, \tag{14}$$

where

$$k_5 = \frac{2k_4}{r_0^2}.$$

This is the Zhuravlev Lesokhin and Templeman equation D5.

2.6. Assumption 1

If the rate controlling step is the transfer across the contracting interface, then only the contracting area of the sphere is important:

$$\frac{\mathrm{d}x}{\mathrm{d}t} = DV_\mathrm{m}C_0 4\pi r^2 = k_6 r^2, \tag{15}$$

where $k_6 = 4\pi DV_\mathrm{m}C_0$,

$$\frac{\mathrm{d}x}{r^2} = k_6\mathrm{d}t. \tag{16}$$

From $(r/r_0)^3 = (1-\alpha)$,

$$r_0^3(1-\alpha) = r^3,$$

take cube roots

$$r_0(1-\alpha)^{+1/3} = r,$$

then

$$r_0^2(1-\alpha)^{2/3} = r^2.$$

Substituting for $\mathrm{d}x$ from Eq. (4), above

$$\therefore \frac{(1/3)r_0(1-\alpha)^{-2/3}}{r_0^2(1-\alpha)^{2/3}}\mathrm{d}\alpha = \frac{(1/3)(1-\alpha)^{-4/3}}{r_0}\mathrm{d}\alpha = k_6\mathrm{d}t.$$

Integrate

$$\tfrac{1}{3r_0}\left(3(1-\alpha)^{-1/3} + c\right) = k_6 t,$$

at $t=0$, $\alpha=0$ and $c=-3$,

$$\frac{1}{r_0}\left(\frac{1}{(1-\alpha)^{1/3}} - 1\right) = k_6 t,$$

$$\left(\frac{1}{(1-\alpha)^{1/3}} - 1\right) = k_7 t, \tag{17}$$

where $k_7 = k_6 r_0$. This is a new equation which it is proposed to label D10.

2.7. Assumption 2

If the interface transfer and diffusion across the product layer both affect the rate,

$$\frac{dx}{dt} = \frac{DV_m C_0 4\pi r^2}{x} = \frac{k_6 r^2}{x}, \tag{18}$$

where $k_6 = 4\pi DV_m C_0$,

$$\frac{x\,dx}{r^2} = k_6\,dt.$$

Substitute for x, dx and r^2

$$\frac{(1/3)r_0^2\left(1-(1-\alpha)^{1/3}\right)(1-\alpha)^{-2/3}d\alpha}{r_0^2(1-\alpha)^{2/3}} = \tfrac{1}{3}\left(1-(1-\alpha)^{1/3}\right)(1-\alpha)^{-4/3}d\alpha = k_6\,dt,$$

$$\tfrac{1}{3}\left((1-\alpha)^{-4/3}-(1-\alpha)^{-3/3}\right)d\alpha = k_6\,dt.$$

Integrate

$$\tfrac{1}{3}\left(3(1-\alpha)^{-1/3} + \ln(1-\alpha) + c\right) = k_6 t,$$

at $t = 0$, $\alpha = 0$ and $c = -3$:

$$(1-\alpha)^{-1/3} - 1 + \tfrac{1}{3}\ln(1-\alpha) = k_6 t,$$

$$\left(\frac{1}{(1-\alpha)^{1/3}} - 1\right) + \frac{1}{3}\ln(1-\alpha) = k_6 t.$$

This is a second new equation which it is proposed to label D11.

2.8. Assumption 3

If the activities of the reactants control the diffusion but the two concentrations affect the rate i.e. second order or diffusion in both directions,

$$\frac{dx}{dt} = \frac{DV_m C_{0A}(1-\alpha)C_{0B}(1-\alpha)}{x} = \frac{k_8(1-\alpha)^2}{x}, \tag{20}$$

where $k_8 = DV_m C_{0A} C_{0B}$,

$$\frac{x\,dx}{(1-\alpha)^2} = k_8\,dt.$$

Substitute

$$\frac{(1/3)(r_0)^2\left((1-\alpha)^{-2/3}-(1-\alpha)^{-1/3}\right)d\alpha}{(1-\alpha)^2} = k_8\,dt,$$

$$\tfrac{1}{3}(r_0)^2\left((1-\alpha)^{-8/3}-(1-\alpha)^{-7/3}\right)d\alpha = k_8\,dt.$$

Integrate

$$\tfrac{1}{3}(r_0)^2\left(\tfrac{3}{5}(1-\alpha)^{-5/3} - \tfrac{3}{4}(1-\alpha)^{-4/3} + c\right)d\alpha = k_8 t,$$

at $t = 0$, $\alpha = 0$ and $3/5 - 3/4 + c = 0$, $c = (15-12)/20 = 3/20$,

$$\therefore\ (r_0)^2\left(\tfrac{1}{5}(1-\alpha)^{-5/3} - \tfrac{1}{4}(1-\alpha)^{-4/3} + \tfrac{1}{20}\right) = k_8 t,$$

or

$$\frac{(r_0)^2}{(1-\alpha)}\left(\frac{1}{5}(1-\alpha)^{-2/3} - \frac{1}{4}(1-\alpha)^{-1/3} + \frac{1-\alpha}{20}\right) = k_8 t,$$

thus

$$\tfrac{1}{5}(1-\alpha)^{-5/3} - \tfrac{1}{4}(1-\alpha)^{-4/3} + \tfrac{1}{20} = k_9 t, \tag{21}$$

where

$$k_9 = \frac{k_8}{(r_0)^2}.$$

This is a third new equation which it is proposed to label D12.

3. Experimentation

The chemical reaction that was being studied was between sodium carbonate and calcium silicate. Analysis of the product by XRD had confirmed the product disodium calcium silicate was formed according to the following equation.

$$Na_2CO_3 + CaSiO_3 \rightarrow Na_2CaSiO_4 + CO_2 \tag{22}$$

As was stated above, the initial kinetic analysis did not give a perfect fit to the D5 equation. A liquid phase was suspected although the temperature was lower than the melting point of either reactant or the product. The lowest melting compound in the system is sodium carbonate which melts at 852°C. It was decided, therefore, to analyse the isothermal data again and include the additional three proposed equations. Also, a method was devised to obtain non-isothermal data on the reaction between liquid sodium carbonate and solid calcium silicate without there being any contact

between the reactants below the melting point of sodium carbonate (852°C). Thus the reaction mechanism for the solid mixture could be compared with the reaction where it was certain that one of the reactants was a liquid. Experimental details follow later. Data was obtained using thermogravimetry when reaction was followed by monitoring the loss of carbon dioxide from sodium carbonate according to Eq. (22) above.

The experiments were carried out in Stanton Redcroft STA1500 simultaneous DTA–TGA equipment coupled to a Commodore PET computer to control the heating rate. The signals from the thermocouples and the balance control electronics were connected to a Yokogawa LR4800 series chart recorder with data logging facilities for four channels of data. The data was stored on a memory card which could be read by the card reading software running on an IBM compatible PC. Data could be recorded at rates between 135 readings per channel per second and one reading per channel per three seconds. The data sampling rate was adjusted in each experiment to give about ten thousand readings, the large number of readings are required to produce acceptable DTA plots which were used for in the liquid–solid experiment. The data was loaded into the technical graphics package Axum to plot the graphs and convert the mass data into the fraction reacted, α. In order to reduce the number of data points to below 1000 for use in the kinetic computer programs the time, temperature and mass data was passed to a Fortran computer program which had been written according to the instructions given by Savitzky and Golay [6]. The program smoothed the data by a polynomial expression operating sequentially on 25 data point at a time. A degree of overlap of the 25 data points was included so that with a combination of overlap and number of iterations the number of data points finally obtained could be adjusted to suit the kinetic computer programs. Thus, the data was reduced by substituting one new data point for 25 original data points and hence produced data with an improved signal to noise ratio without distorting the data in any way. The resulting file was analysed by the appropriate computer programs for isothermal or non-isothermal data.

Non-isothermal experiments were carried out at different heating rates. Mass loss data was converted into alpha values and analysed by the classical method of Škvára and Šesták [7]. Additional experiments were carried out at constant temperature and analysed by the reduced time plots [2]. This method could not be used in the study of the liquid sodium carbonate and solid calcium silicate experiment because it was not possible to hold the two substances apart and prevent any reaction until the sodium carbonate had melted.

4. Experimental details

A modification to the typical thermogravimetric experiment was introduced to measure the mass loss resulting from the reaction of liquid sodium carbonate and solid calcium silicate. For this to work it was necessary to weigh the two reactants accurately and hold them apart until the sodium carbonate had melted. A method of combining the two, quickly, at a known temperature had to be devised. This was achieved by the following procedure. A short length, (about 100 mm), of fine platinum wire (0.01 inches diameter) was heated to red heat in a Bunsen flame. Whilst at red heat it was rapidly dipped into a small tube of sodium carbonate so that some of the material adhered to the platinum wire. The wire was re-heated so that the sodium carbonate, adhered to the wire, melted and formed a small bead on the end of the wire. The first bead formed on the wire was a dark colour, possibly due to impurities from the platinum wire. The first bead was therefore removed by shaking the wire when hot. This was also, to allow for any sodium carbonate which might remain on the wire after the bead had dropped into the reaction mixture. The wire was then weighed and a new bead formed as before. By repeating the process it was possible to obtain a bead of 6.9 mg which was the same as the mass of sodium carbonate used in the previous solids mixture experiments. It was important to ensure that the bead was positioned exactly on the end of the wire. This was easily done since the bead was small enough not to fall off the end even when the sodium carbonate was molten. The platinum wire was then cut about 20 mm from the bead. In order to be sure that the bead would fall off the wire when molten, a ring of thick, close fitting, platinum wire was fabricated and threaded on to the wire to rest on the bead. The mass of the platinum ring would force the sodium carbonate to

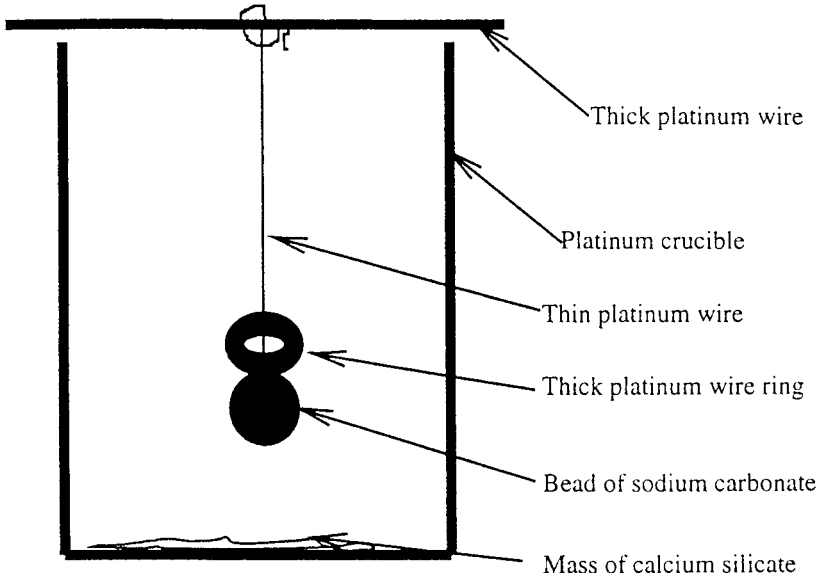

Fig. 3. Crucible assembly for liquid–solid reaction.

fall into the crucible when the bead melted, refer to Fig. 3.

6 mg of calcium silicate was then weighed into the platinum crucible. The bead of sodium carbonate, with the ring of platinum resting on it, was suspended over the calcium silicate by wrapping the end of the thin platinum wire round a short length of thicker platinum wire which bridged the top of the crucible. The assembled apparatus is shown in Fig. 3. The crucible and assembly were then placed in the thermobalance which was programmed to heat at 20°C/min up to 1200°C. When the temperature reached the melting point of sodium carbonate, the mass of the platinum ring forced the molten sodium carbonate onto the calcium silicate. TG and DTA readings were recorded every second. The TG curve was compared with the curve from the mixture of the solid materials.

5. Results

The TG curve was significantly different at the lower temperatures to the earlier experiments where the sodium carbonate was mixed in with the calcium silicate. In the liquid sodium carbonate experiment there was no mass loss up to 850°C, a rapid mass loss occurred at 858°C which gradually slowed down at about 900°C. The mass loss began to increase above 1000°C in a manner similar to the earlier experiments. The DTA curve showed a major endothermic peak at 863°C which on careful inspection on an expanded temperature scale, appeared to be a combination of two peaks (Fig. 4). Interestingly, the DTA showed the commencement of the endotherm was at 820°C, and at exactly 858°C there was a discontinuity in the curve. This is consistent with the sodium carbonate melting and falling onto the calcium silicate. It is surprising that the instrument was sensitive enough to detect the melting of the sodium carbonate whilst suspended on the platinum wire and not in direct contact with the thermocouple. The multiple endotherm appears to consist of two overlapping peaks at 862°C and 872°C.

The TG and DTA plots over the limited temperature range 800–950°C were shown in (Fig. 4). Fig. 5 shows the DTA scatter plot of the data over the whole of the temperature range up to 1200°C. The endothermic peak at 862°C shows the discontinuity almost halfway up the low temperature side of the endothermic peak after which the data points are more widely spaced as the temperature differential changes more rapidly

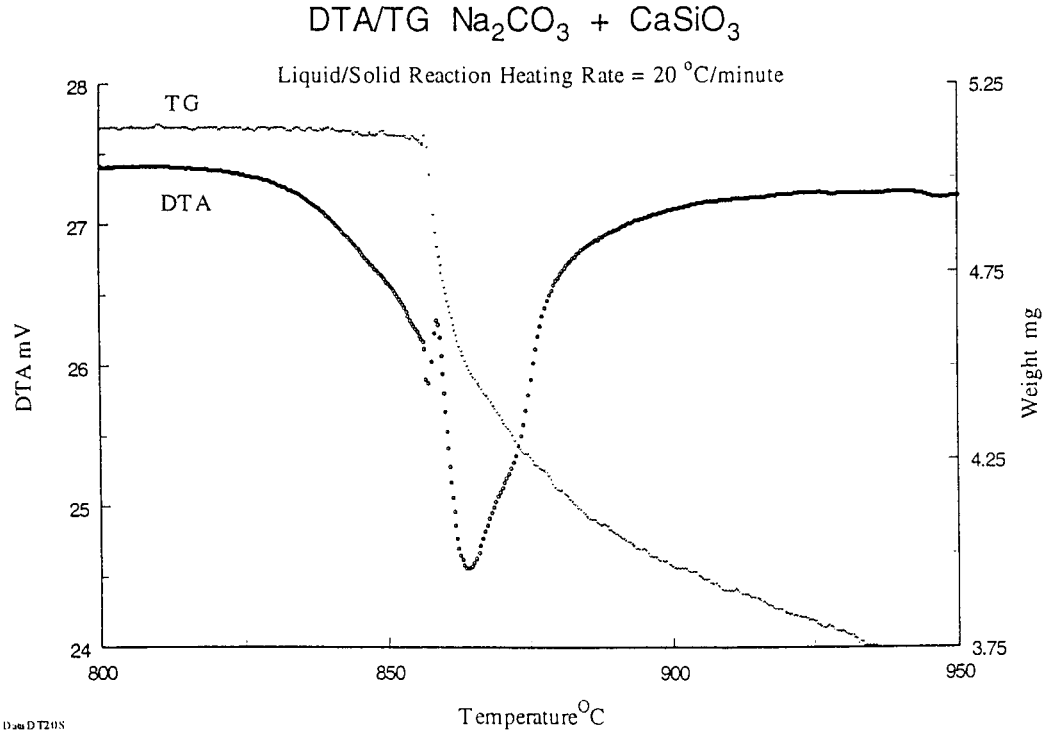

Fig. 4. DTA and TG plots over the temperature range 800–950°C.

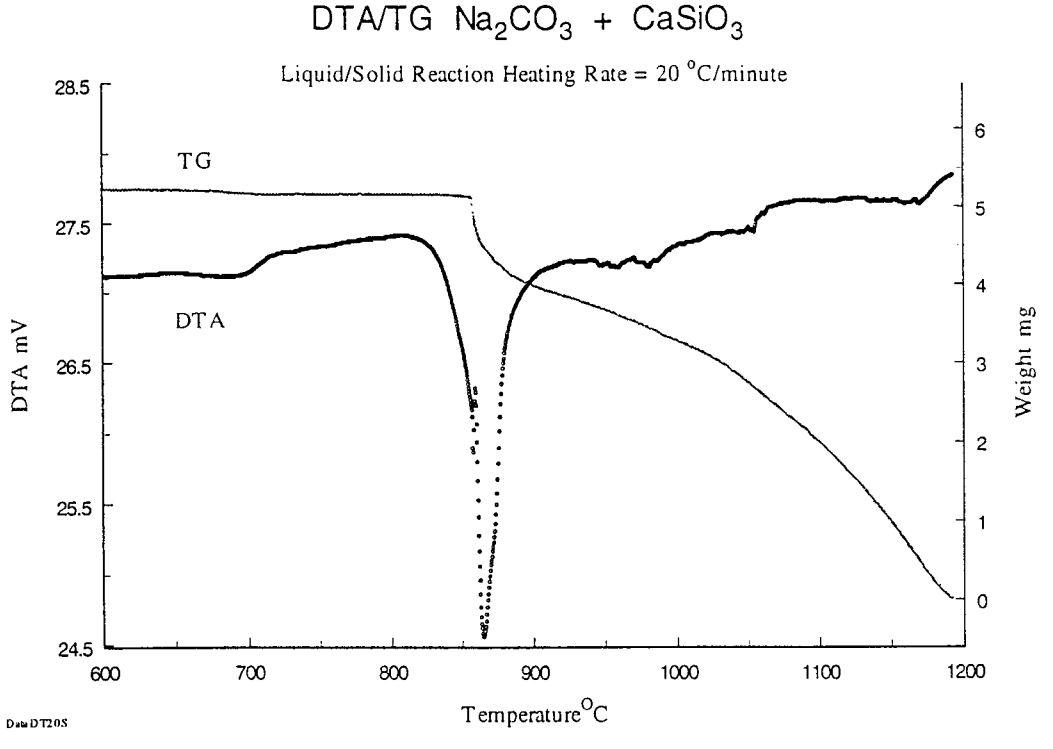

Fig. 5. DTA and TG plots over the temperature range 600–1200°C.

after the liquid sodium carbonate contacts the calcium silicate. It can also be seen that the DTA peak is a compound peak consisting of at least two peaks. One peak may be attributed to the melting of sodium carbonate, the second peak may be the reaction between sodium carbonate and calcium silicate since the reaction is expected to be endothermic.

6. Data analysis

Thermogravimetric data from the experiment was analysed by computer to determine the rate equation, Activation energy and Arrhenius constants. The computer program was based on the non-isothermal method developed by Šesták. All of the known rate equations, except the Prout–Tompkins as mentioned above, were included as possible mechanisms including the three new equations derived above. The total number of equations input was 28, the equation not used was the Prout–Tompkins equation i.e. $kt = \ln(\alpha/1-\alpha)$, which cannot be made to work with Šesták's method of analysis. It was not expected that this equation would be a possible solution since the Prout–Tompkins is a sigmoid type equation. The optimum rate equation was selected by the program using a statistical analysis which produced the least deviation from perfect data generated from the standard equations.

The initial part of the reaction ($\alpha = 0$–0.25) and the middle part of the reaction ($\alpha = 0.2$–0.7) gave an equal fit to two equations, F2 and D12, one of the new equations. The computer programs calculated correlation coefficient for each equation tested and hence it was possible to determine which equation was the closest fit. A perfect fit gives a value of 1.0000. The correlation for each equation was 0.927 (59 data points) and 0.989 (450 data points) respectively. Type F2 is of second order based on concentration. Equation D12 is one of the new equations derived above. As was mentioned previously, the analysis carried out in the M.Sc. Thesis [1], using solid mixtures, had identified the Zhuravlev et al. a D5 type diffusion controlled equation. However, a re-analysis of the same data but now including the three new equations, identified function D12 as the equation with the best correlation with the data.

7. Discussion

The three new equations were derived from the assumption that one of the reactants was surrounded in a sea of liquid. Thermogravimetric data from the liquid sodium carbonate and solid calcium silicate experiment tends to support this idea and identifies the D12 equation as a possible solution. However, analysis of non-isothermal thermogravimetric data from experiments carried out with solid reactants at temperatures below the melting point of sodium carbonate produced agreement with the same equation. Several isothermal experiments carried out in the temperature range 720–750°C and analysed by the method Sharp et al. [2] of reduced time plots produces the same answer (refer to Figs. 6–11). This method of analysis was most convincing since equation D12 was clearly of greater deceleratory nature than any other equation tested.

The conclusions drawn from this are that a liquid phase is produced as soon as a small amount of product is formed from the reaction. The product of the reaction then forms an eutectic melt with some of the un-reacted sodium carbonate. Obviously, this cannot occur until there is sufficient product formed to give a eutectic melt at a temperature at or below the experimental temperature. This is not so easily observed in non-isothermal experiments where the temperature is continuously rising unless more than one heating rate is compared. The temperature at which the first liquid phase appears depends on how much product is formed. Increasing quantities of product will further depress the melting point of the eutectic until such a point as the amount of product formed and the un-reacted sodium carbonate in the correct proportions to give the minimum eutectic melt temperature. Further reaction, producing more product, will then cause the eutectic melt temperature to rise until such a point as the mixture becomes solid again. This explains the observations in the experiments where the mass loss for each heating rate plotted against temperature produced curves which crossed. This kind of behavior could explain the strongly deceleratory nature of the reaction mechanism and would explain why the change in mechanism occurred at a temperature dependent on the heating rate in the original non-isothermal experiments. A slower heating rate would allow more product to be formed at the

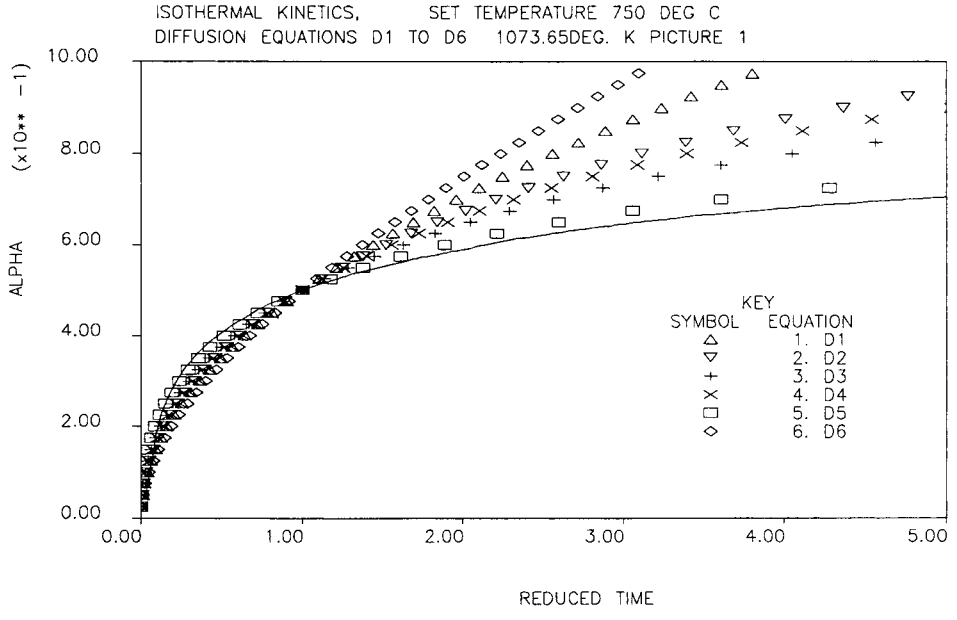

Fig. 6.

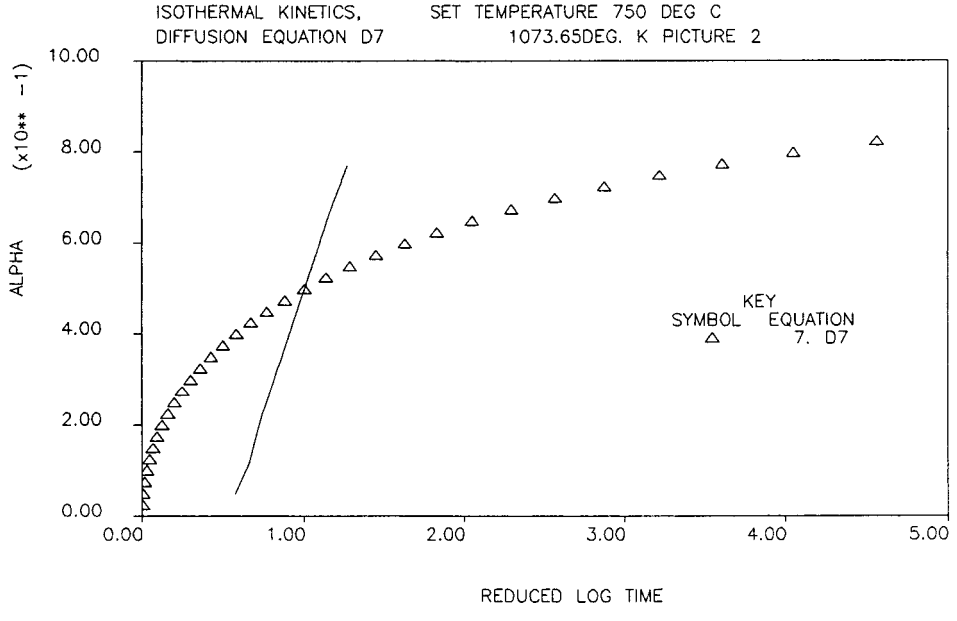

Fig. 7.

lower temperatures which would give a lower eutectic melt and hence a change in mechanism at a lower temperature. Fig. 12 shows the plots of the results of the isothermal experiments. From the graph the activation energy and the pre-exponential factor can be calculated by the following.

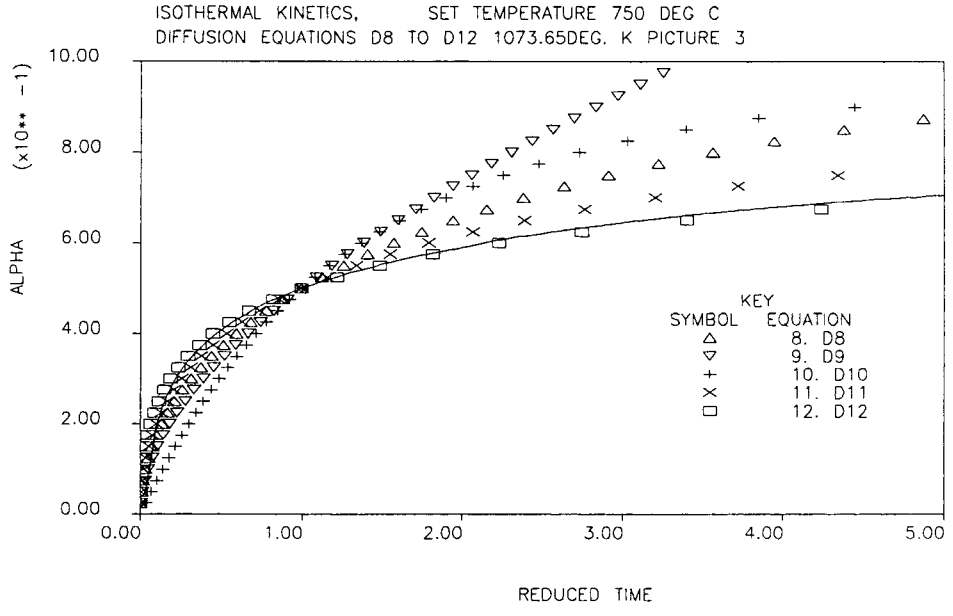

Fig. 8.

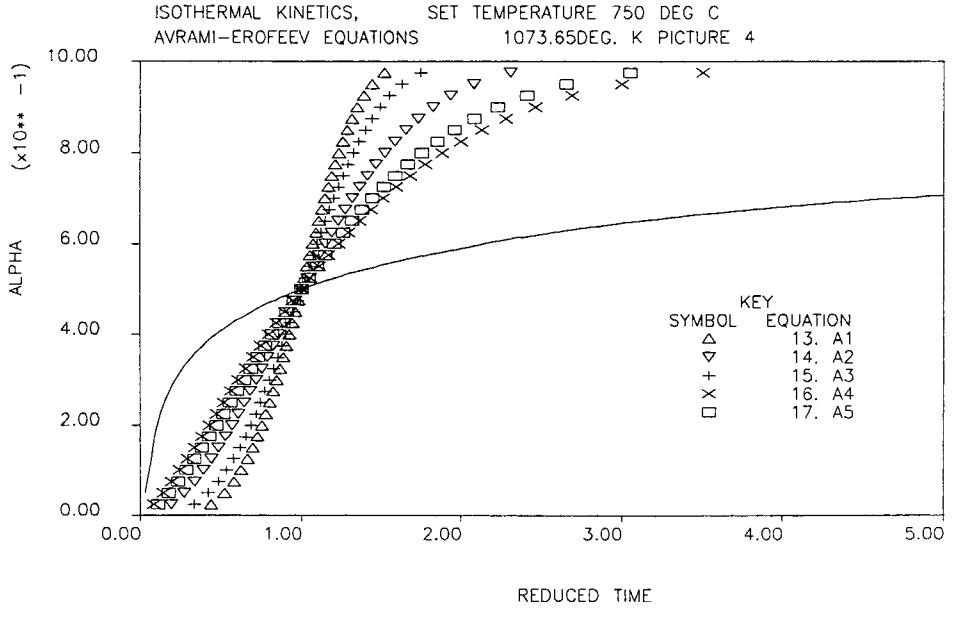

Fig. 9.

Slope $= -E/R$, where E is the activation energy and R is the gas constant.
Intercept $= \log A$, where A is the pre-exponential factor (Arrhenius constant).

Slope $= -17763 = -E/8.314$, $E = \text{Slope} \times 8.314 = 148$ kJ/mol.
Intercept $= \log A = 12.542$, $A = 3.4833 \times 10^{12}\ \text{s}^{-1}$.

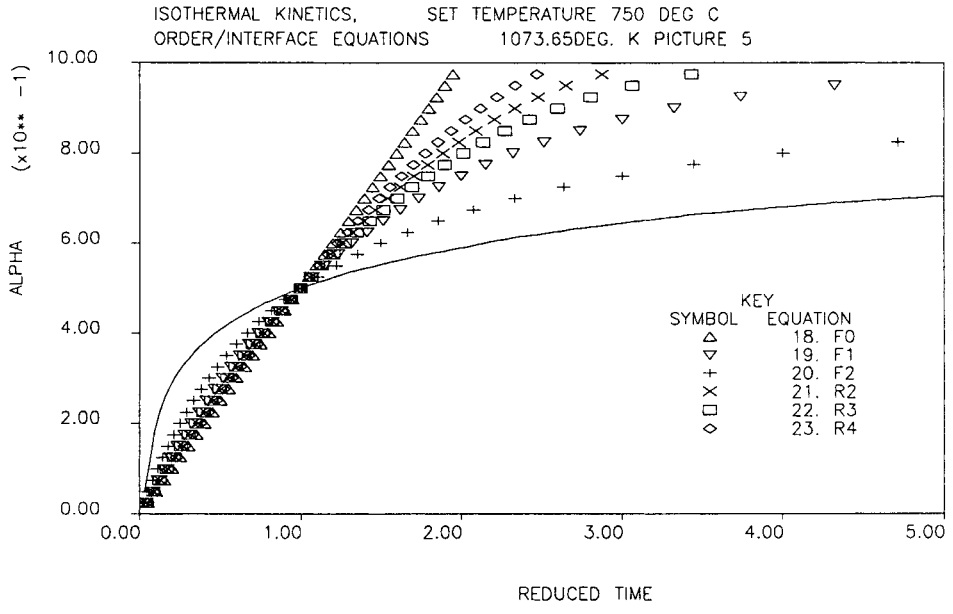

Fig. 10.

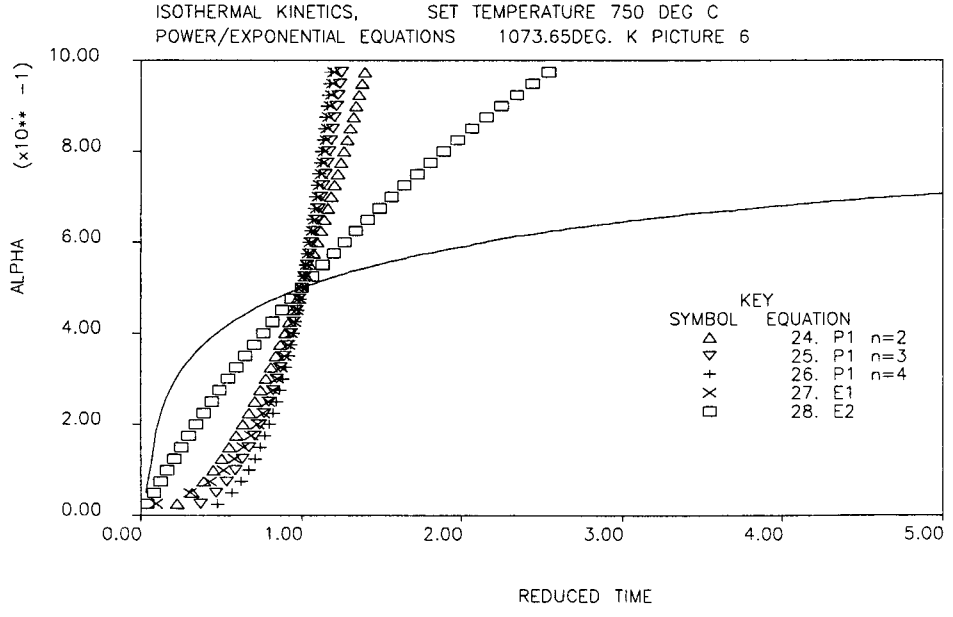

Fig. 11.

Prior to the development of the D12 equation the D5 rate equation was the equation with the closest fit to the data. This gave the following results.

$E = 111$ kJ/mol and $A = 6.442 \times 10^7$ s^{-1}. The differences are quite large considering that, initially, that the D5 equation was by far the closest fit to the data

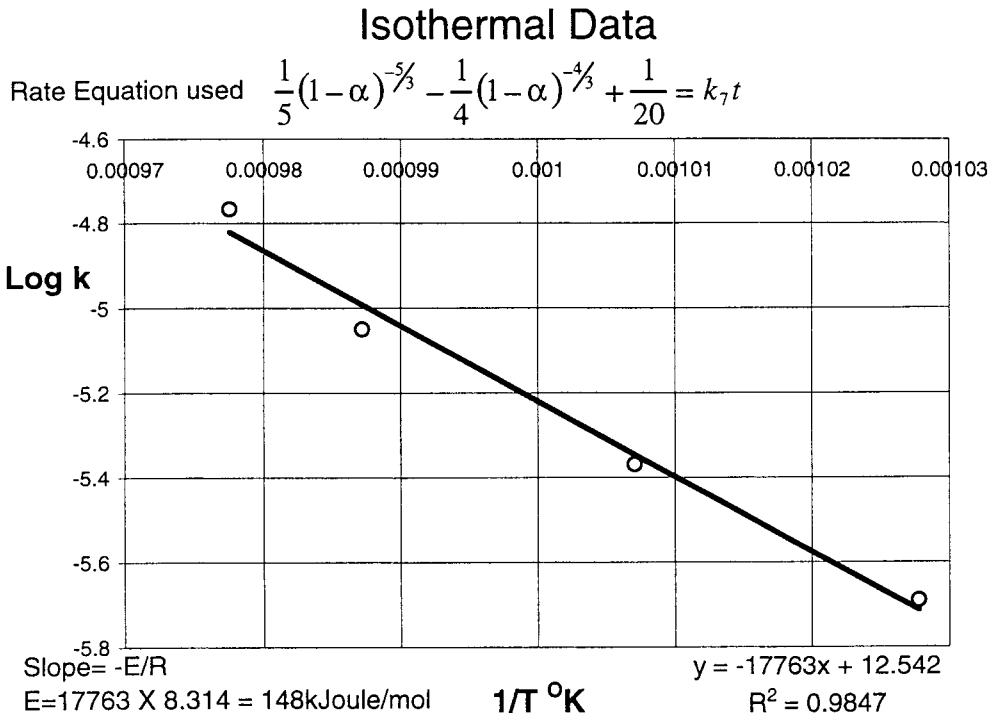

Fig. 12.

than any other equation and so appeared to be a reasonable choice of rate equation.

8. Conclusions

The reaction of sodium carbonate and calcium silicate is a complex reaction involving three different mechanisms dependent on the time and temperature. The initial reaction mechanism at temperatures below the melting point of sodium carbonate does not follow a solid–solid diffusion controlled mechanism but follows a solid–liquid mechanism. This suggests that the formation of reaction products give rise to an eutectic melt with one of the reactants, probably the sodium carbonate. The comparison of the liquid and solid experiment with the solid mixture experiments shows good agreement and identifies the same rate equation. This equation is one of three proposed diffusion controlled rate equations that were derived from assumptions that a spherical solid is suspended in a sea of molten reactant. Validation of this equation is suggested since this same rate equation is preferred in the solid mixture experiments as is in the liquid–solid experiment. It may also appear that these experiments give some weight to the argument that it is possible to distinguish the rate equation and calculate the activation energy from a single non-isothermal experiment. For this particular reaction, this is true since several isothermal experiments identified the same rate equation as the single non-isothermal experiment. However, this reaction showed an extreme deceleratory nature, much more than any of the alternatives, which made identification easier than it might have been had the deceleratory nature of the experiment been less extreme.

References

[1] C.F. Dickinson, M.Sc. Thesis, University of Salford, 1995.
[2] J.H. Sharp, G.H. Brindley, B.N. Narahari Achar, J. Am. Ceram. Soc. 49 (1966) 379–382.

[3] V.F. Zhuravlev, I.G. Lesokhin, R.G. Templeman, J. Appl. Chem. (USSR) 21 (1948) 887.
[4] W. Komatsu, T. Uemura, Ziet. Physik. Chem., Neue Folge 72 (1970) 59–75.
[5] J. Šesták, V. Satava, W.W. Wendlandt, Thermochim. Acta 7 (1973) 333.
[6] A. Savitzky, M.J.E. Golay, Analytic. Chem. 36 (1964) 1627–1639.
[7] F. Škvára, J. Šesták, J. Thermal Anal. 8 (1975) 477–489.